Conference paper

Seungjib Yum, Tae Kyu An, Xiaowei Wang, Mohammad Afsar Uddin, Thanh Luan Nguyen, Shuhao Xu, Hwasook Ryu, Yu Jin Kim, Sungu Hwang, Chan Eon Park* and Han Young Woo*

Thienothiophene-benzotriazole-based semicrystalline linear copolymers for organic field effect transistors

Abstract: A series of thienothiophene-benzotriazole-based semicrystalline copolymers, **PTTBTz**, **PTTBTz-F**, and **PTTBTz-OR**, were synthesized by considering chain linearity, planarity and inter-chain packing by virtue of non-covalent attractive interaction. Fluorine and alkoxy substituents were introduced to modulate the intra- and inter-chain coulombic interactions and crystalline ordering. The fluorine and alkoxy-substituted **PTTBTz-F** and **PTTBTz-OR** showed pronounced inter-chain packing with edge-on orientation confirmed by UV-vis absorption and X-ray diffraction measurements. The well-resolved diffraction patterns were obtained for **PTTBTz-F** and **PTTBTz-OR**, showing (100)~(500) inter-lamellar scattering peaks (d-spacing, 17~18 Å) in the out-of-plane direction and a π-π stacking peak (d-spacing, 3.5~4.1 Å) in the in-plane direction. Organic field effect transistor (OFET) devices were fabricated with a bottom gate and top contact geometry. **PTTBTz-F** ($\mu_h = 4.49 \times 10^{-2}$ cm^2 V^{-1} s^{-1}, on/off ratio = 1.13×10^7) and **PTTBTz-OR** ($\mu_h = 8.39 \times 10^{-3}$ cm^2 V^{-1} s^{-1}, on/off ratio = 2.98×10^4) showed nearly 3 and 2 orders of magnitude higher hole mobility upon annealing at 305 and 260 °C, with compared to the unsubstituted **PTTBTz**.

Keywords: ICFPAM-2013; optoelectronics; organic field-effect transistors; semiconductors; X-ray diffraction.

DOI 10.1515/pac-2014-0205

Introduction

Solution-processable organic semiconductors have attracted growing attention for potential applications in printed and flexible electronics such as organic field-effect transistors (OFETs), etc. [1–3]. Significant pro-

Article note: A collection of invited papers based on presentations at the 12th International Conference on Frontiers of Polymers and Advanced Materials (ICFPAM 2013), Auckland, New Zealand, 8–13 December 2013.

***Corresponding authors: Chan Eon Park,** POSTECH Organic Electronics Laboratory, Polymer Research Institute, Department of Chemical Engineering, Pohang University of Science and Technology, Pohang, Gyungbuk 790-784, South Korea, Tel.: +82-54-279-2269, Fax: +82-54-279-8298, E-mail: cep@postech.ac.kr; and **Han Young Woo,** Department of Nanofusion Engineering, Department of Cogno-Mechatronics Engineering, Pusan National University, Miryang, 627-706, Republic of Korea, Tel.: +82-55-350-5300, Fax: +82-55-350-5279, E-mail: hywoo@pusan.ac.kr

Seungjib Yum, Xiaowei Wang, Mohammad Afsar Uddin, Thanh Luan Nguyen, Shuhao Xu, Hwasook Ryu and Sungu Hwang: Department of Nanofusion Engineering, Department of Cogno-Mechatronics Engineering, Pusan National University, Miryang, 627-706, Republic of Korea

Tae Kyu An and Yu Jin Kim: POSTECH Organic Electronics Laboratory, Polymer Research Institute, Department of Chemical Engineering, Pohang University of Science and Technology, Pohang, Gyungbuk 790-784, South Korea

gresses have been made in molecular design and device architectures to realize OFETs showing comparable or exceeding performance than amorphous silicon-based ones [4–6]. Conjugated polymers offer great advantages with good mechanical flexibility and large-area solution processibility. However, poor inter-chain packing of π-conjugated polymers hampers the effective charge transport with the lower field-effect mobility, relative to small molecules. Rational molecular design and synthesis of π-conjugated polymers are required to enhance the intermolecular interactions and crystalline ordering of polymeric chains without losing solution processibility. To improve inter-chain orientation, polymeric chain planarity, curvature, intra- and intermolecular interactions should be considered carefully [7, 8]. Various combinations of electron (e)-donor (i.e., cyclopentadithiophene, thiophene, thienothiophene, etc.) and e-acceptor units (benzothiadiazole, diketopyrrolopyrrole, isoindigo, etc.) resulted in field-effect mobility as high as 12 $cm^2 V^{-1} s^{-1}$ [4, 5, 9–11].

Careful choices of side chains are also important to increase solubility with minimized perturbation in inter-chain packing. Alkoxy substituents on the e-rich donor segment destabilizes the highest occupied molecular orbital (HOMO), deteriorating oxidational device stability [12, 13]. In contrast, inserting the alkoxy chains onto the e-poor acceptor segment is an effective strategy with little effects on the HOMO level. There is an additional conformational locking effect to induce a planar chain conformation by way of electrostatic interactions between partially positive sulfur and electronegative oxygen atoms in the thiophene derivatives-containing structures [13]. In addition, fluorine substitution suggests an effective way to increase the crystalline ordering with thermal stability through C-F···H, F···S and C-F···π_F non-covalent attractive interactions [5, 14].

Here, we report the synthesis of three thienothiophene-benzotriazole alternating copolymers and characterization of their OFET device properties. The benzotriazole moiety offers the alkyl chain substitution on the central nitrogen (which is away from the π-conjugated backbone with little steric hindrance) as well as two functionalizable sites on 5- and 6 positions on the benzene ring. Three benzotriazole derivative moieties, N-alkylylated (BTz), fluorinated (BTz-F) and alkoxy substituted benzotriazole (BTz-OR), were polymerized with thienothiophene, resulting three crystalline linear copolymers of poly[2-(2-hexyldecyl)-4-(thieno[3,2-*b*]-thiophen-2-yl)-2*H*-benzo[*d*][1,2,3]triazole] (**PTTBTz**), poly[2-(2-hexyldecyl)-5,6-difluoro-4-(thieno[3,2-*b*]thiophen-2-yl)-2*H*-benzo[*d*][1,2,3]triazole] (**PTTBTz-F**) and poly[2-octyl-5,6-bis(octyloxy)-4-(thieno[3,2-*b*]thiophen-2-yl)-2*H*-benzo[*d*][1,2,3]triazole] (**PTTBTz-OR**). The alkoxy- and fluorine-substituted **PTTBTz-OR** and **PTTBTz-F** showed pronounced inter-chain packing with edge-on orientation confirmed by UV-vis absorption and X-ray diffraction measurements. The fluorinated **PTTBTz-F** showed nearly 3 orders of magnitude higher hole mobility ($\mu_h = 4.49 \times 10^{-2}$ $cm^2 V^{-1} s^{-1}$, on/off ratio = 1.13×10^7) upon annealing at 305 °C with compared to the non-fluorinated one (**PTTBTz**). The alkoxy-substituted **PTTBTz-OR** enhanced hole mobility up to 2 orders of magnitude ($\mu_h = 8.39 \times 10^{-3}$ $cm^2 V^{-1} s^{-1}$, on/off ratio = 2.98×10^4) than that of **PTTBTz** upon annealing at 260 °C. The detailed structure–property relationship for the three BTz-based polymers will be discussed.

Experimental section

Materials

All chemical reagents were purchased from Aldrich, Tokyo Chemical Industry and Junsei Chemical and used without further purification. The intermediates and monomers (BTz, BTz-F, BTz-OR) were prepared by modifying the previously reported procedures [15–21].

Measurements

^1H and ^{13}C NMR spectra were recorded on a JEOL (JNM-AL300) FT NMR system operating at 300 and 75 MHz, respectively. The polymerization reaction was done by using a microwave reactor (Biotage Initiator™). The

number- and weight-average molecular weights of the polymers were determined relative to polystyrene standard with *o*-dichlorobenzene as an eluent at 80 °C using gel permeation chromatography (GPC) equipped with a Waters 1515 isocratic HPLC pump, a temperature control module, and a Waters 2414 refractive index detector. Thermogravimetric analysis (TGA) and differential scanning calorimetry (DSC) measurements of the polymers were performed using a TA instrument TGA 2050 thermogravimetric analyzer and DSC Q200 under a nitrogen atmosphere at a heating and cooling rate of 10 °C/min. UV/Vis absorption spectra were measured using a Jasco (V-630) spectrophotometer. Cyclic voltammetry data were measured on a Versa STAT 3 (Princeton Applied Research) with a three-electrode cell in 0.1 M tetrabutylammonium tetrafluoroborate (Bu_4NBF_4) in CH_3CN at a scan rate of 50 mV/s. A platinum electrode coated with a thin polymer film was used as the working electrode and platinum and $Ag/AgNO_3$ electrodes were used as the counter- and reference-electrodes, respectively. All measurements were calibrated against an internal standard of ferrocene (Fc), the ionization potential (IP) value of which was assumed to be −4.78 V for the Fc/Fc^+ redox system. Atomic force microscopy (AFM, Multimode IIIa, Digital Instruments) was operated in tapping mode to acquire the surface images of polymer films. X-ray diffraction (XRD) studies were performed at the 5A beam line at the Pohang Accelerator Laboratory (PAL), Korea.

OFET fabrication

Electrical properties were characterized in a top-contact OFET configuration using a 300 nm thick SiO_2 dielectric on a highly doped n-Si substrate as the gate electrode. The substrate was cleaned with piranha solution and ozone-treated for 20 min. Cleaned substrates were treated with octadecyltrichlorosilane (ODTS) in toluene for 90 min at room temperature and the semiconducting polymer films were spin-coated at 6000 rpm from a 0.2 wt % solution (**PTTBTz**: chloroform, **PTTBTz-F** and **PTTBTz-OR**: chlorobenzene) with a nominal thickness of 40 nm. The film thickness was measured using a surface profiler (Alpha Step 500, Tencor). Gold source and drain electrodes (thickness ~100 nm) were evaporated on top of the semiconductor layers using a shadow mask. For all measurements, the channel length (L) and width (W) were 160 and 1600 μm, respectively. The OFET devices were annealed at various temperatures for 10 min under a nitrogen atmosphere. The electrical characteristics of the OFETs were measured under ambient conditions using Keithley 2400 and 236 source/measure units. Field-effect mobility was extracted in the saturation regime from the slope of the source–drain current using the equation, $I_{DS} = (WC_i/2L)\mu(V_G - V_{th})^2$, where I_{DS} is the drain current, C_i is the capacitance per unit area of dielectric, μ is the field-effect mobility, and V_{th} is the threshold voltage.

Synthesis of polymers

Poly[2-(2-hexyldecyl)-4-(thieno[3,2-*b*]thiophen-2-yl)-2*H*-benzo[*d*][1,2,3]triazole] (PTTBTz)

2,5-Bis(trimethylstannyl)thieno[3,2-*b*]thiophene (303 mg, 0.651 mmol), BTz (421 mg, 0.651 mmol), $Pd_2(dba)_3$ (17.9 mg, 19.5 μmol) and tri(*o*-tolyl)phosphine (23.7 mg, 78.2 μmol) were dissolved in dry chlorobenzene (4 mL). The mixture was heated at 100 °C for 15 min, 120 °C for 15 min, and 140 °C for 60 min in a microwave reactor. 2-Bromothiophene (1 equiv.) and 2-(tributylstannyl)thiophene (2 equiv.) were sequentially added to the reaction mixture as an end-capper and heated at 140 °C for 10 min. The reaction mixture was allowed to cool down to room temperature and then precipitated into a MeOH/HCl mixture (250 mL/10 mL). The polymer was filtered and purified by Soxhlet extraction with acetone (12 h), n-hexane (12 h) and chlorobenzene (6 h). The chlorobenzene fraction was precipitated into MeOH and recovered by filtration. The final product was obtained after drying under vacuum at 50 °C. Yield: 237 mg (65.7 %). ^{1}H NMR (300 MHz, $CDCl_3$, ppm): δ 8.98

(br, 4H), 4.87 (br, 2H), 2.50 (br, 1H), 2.00–0.80 (br, 30H). Number-average molecular weight (GPC, $C_6H_4Cl_2$): M_n = 11.6 kDa [polydispersity index (PDI) = 4.21].

Poly[2-(2-hexyldecyl)-5,6-difluoro-4-(thieno[3,2-*b*]thiophen-2-yl)-2*H*-benzo[*d*][1,2,3] triazole] (PTTBTz-F)

2,5-Bis(trimethylstannyl)thieno[3,2-*b*]thiophene (388 mg, 0.833 mmol), **BTz-F** (448 mg, 0.833 mmol), $Pd_2(dba)_3$ (22.9 mg, 25 μmol) and tri(*o*-tolyl)phosphine (30.4 mg, 100 μmol) were dissolved in dry toluene (4 mL). **PTTBTz-F** was prepared by following the similar procedure as for **PTTBTz**. The polymer was purified by sequential Soxhlet extraction with acetone (12 h), n-hexane (12 h) and $CHCl_3$ (6 h). The $CHCl_3$ fraction was precipitated into MeOH and recovered by filtration. Yield: 340 mg (78.8 %). Number-average molecular weight (GPC, $C_6H_4Cl_2$): M_n = 2.7 kDa (PDI = 1.45). ^{1}H NMR could not be measured due to poor solubility.

Poly[2-octyl-5,6-bis(octyloxy)-4-(thieno[3,2-*b*]thiophen-2-yl)-2*H*-benzo[*d*][1,2,3] triazole] (PTTBTz-OR)

2,5-Bis(trimethylstannyl)thieno[3,2-*b*]thiophene (303 mg, 0.651 mmol), BTz-OR (420 mg, 0.651 mmol), $Pd_2(dba)_3$ (17.9 mg, 19.5 μmol) and tri(*o*-tolyl)phosphine (23.7 mg, 78.2 μmol) were dissolved in dry chlorobenzene (4 mL). **PTTBTz-OR** was synthesized by following the similar procedure as for **PTTBTz**. The polymer was purified by sequential Soxhlet extraction with acetone (12 h), n-hexane (12 h) and chlorobenzene (6 h). The chlorobenzene fraction was precipitated into MeOH and recovered by filtration. Yield: 237 mg (58.2 %). ^{1}H NMR (300 MHz, $C_6D_4Cl_2$, ppm): δ 9.00 (br, 2H), 4.71 (br, 2H), 4.28 (br, 4H), 2.11 (br, 6H), 1.28 (br, 30H), 0.87 (br, 9H). Number-average molecular weight (GPC, $C_6H_4Cl_2$): M_n = 5 kDa (PDI = 1.24).

Results and discussion

Molecular design and synthesis

Electron-rich thienothiophene and electron-deficient BTz units were combined to build a linear and planar D-A copolymers (Scheme 1). A bond angle (180°) at the thienothiophene and BTz linkage induces a linear polymeric chain which facilitates the inter-chain molecular ordering. Small degree of chain curvature has shown to enhance the carrier mobility through effective inter-chain interaction [11]. As shown in Scheme 1, all polymers were designed by considering the chain planarity and intermolecular packing by virtue of intra-/inter-chain non-covalent attractive interactions (N···H, N···S interactions for **PTTBTz**; F···S, F···H-C, C-F···π_F, N···H, N···S interactions for **PTTBTz-F**; S···O, O···H, N···H, N···S interactions for **PTTBTz-OR**) [5, 13, 14]. Dihedral angles between the thienothiophene and benzotriazole rings were calculated to be 0 ~ 10 ° by density functional theory (DFT) calculation (B3LYP/6-31G** level). Fluorine substitution does not increase a torsional angle because of its small val der Waals radius (1.35 Å) and attractive intra-chain coulomb interactions (i.e., F···S, F···H-C, N···H, N···S, etc.), with compared to unsubstituted **PTTBTz** (dihedral angle = 0 °). Introduction of the alkoxy chain on the benzotriazole moiety increases a dihedral angle slightly (~10 °) where the electrostatic intra-molecular interaction between partially positive sulfur (δ^+) and electronegative oxygen (δ^-) atoms facilitates the chain planarity [13]. In addition, the two energy minimum conformations are expected to repeat randomly in the polymeric backbone for the polymers, as displayed in Scheme 1b. To resolve the solubility issue, a 2-hexyldecyl group was introduced onto the benzotriazole moiety (BTz and BTz-F) or two octyloxy and n-octyl chains were attached (BTz-OR) [21]. Polymerization of the corresponding BTz monomers (BTz, BTz-F, BTz-OR) with 2,5-bis(trimethylstannyl)thieno[3,2-*b*]thiophene by Stille coupling using $Pd_2(dba)_3$/tri(*o*-tolyl)

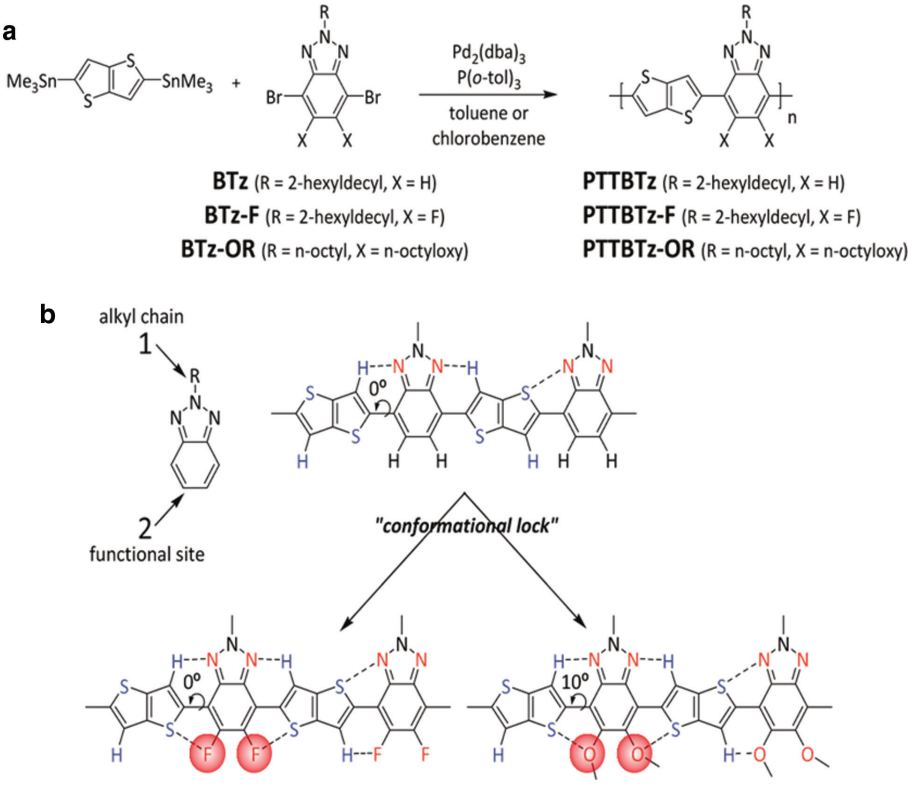

Scheme 1 (a) Synthetic routes and (b) schematic non-covalent attractive interactions in BTz-based polymers.

phosphine as a catalyst, afforded three poymers, **PTTBTz**, **PTTBTz-F** and **PTTBTz-OR** in 60–80 % yields. **PTTBTz-F** showed a limited solubility but **PTTBTz** and **PTTBTz-OR** showed moderate solubility in chlorinated organic solvents, i.e., chlorinated benzenes and chloroform, etc. The molecular weight (2.7~11.6 kDa) and thermal properties are summarized in Table 1. **PTTBTz** and **PTTBTz-F** showed no weight loss up to ~420 °C in TGA thermograms (Fig. S1). The relatively low decomposition temperature (T_d = 331 °C) of **PTTBTz-OR** is due to the break-up of the octyloxy side chains. No phase transitions were observed in the DSC measurements up to ~300 °C.

Optical and electrochemical property

Normalized UV-vis absorption spectra of the polymers in solution and film with/without thermal annealing are shown in Fig. 1. The absorption maxima were measured at 545~575 nm, showing well-resolved vibronic structures. Upon thermal treatments with changing the annealing temperature, the vibronic shoulder peak at ~605 nm was intensified for **PTTBTz-F** and **PTTBTz-OR**, which is consistent with our assumption of the

Table 1 Physical, thermal, optical and electrochemical properties of polymers.

Polymer	M_n (kDa)[a]/PDI	T_d (°C)[b]	E_g (eV)[c]	HOMO (eV)[d]	LUMO (eV)[e]
PTTBTz	11.6/4.21	423	1.82	−5.19	−3.37
PTTBTz-F	2.7/1.45	419	1.91	−5.33	−3.42
PTTBTz-OR	5/1.24	331	1.92	−5.03	−3.11

[a]Number-average molecular weight. [b]Decomposition temperature with 5 % weight loss in TGA measurements. [c]Optical band gap was estimated from the absorption onset in as-casted film. [d]HOMO level was estimated from the first oxidation potential relative to ferrocene/ferrocenium (Fc/Fc^+) system. [e]LUMO level was calculated using the HOMO energy level and optical band gap. ($E_{LUMO} = E_{HOMO} + E_g$).

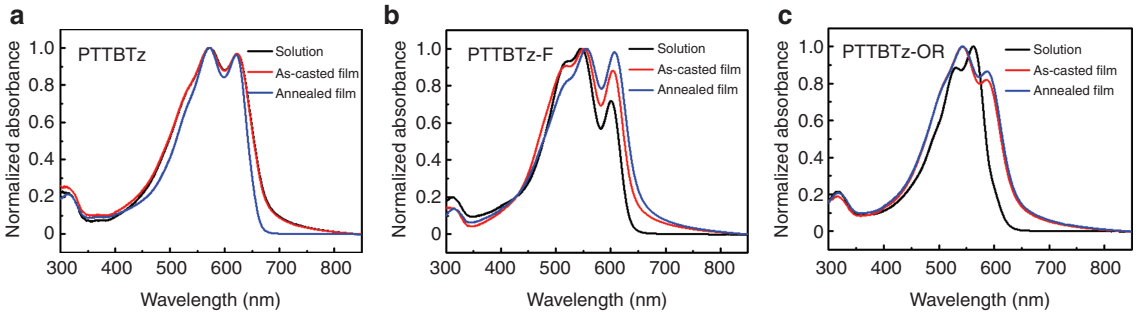

Fig. 1 Normalized UV-vis absorption spectra of (a) **PTTBTz**, (b) **PTTBTz-F** and (c) **PTTBTz-OR** in solution and film with/without thermal annealing at 130, 280, and 230 °C, respectively.

efficient intermolecular interaction and inter-chain packing by way of non-covalent attractive interactions (Fig. S2). The alkoxy and fluorine substitution does not increase the torsional angle of the polymeric chain. The optical band gap was determined to be 1.82 eV for **PTTBTz** and ~1.9 eV for **PTTBTz-F** and **PTTBTz-OR**. The small band gap of the BTz-based polymers is due to the intramolecular charge transfer (ICT) interaction from the thienothiophene to benzotriazole segments.

Cyclic voltammograms of the polymers in thin film were measured to estimate their Frontier orbital energy levels (Fig. S3, Table 1). All polymers displayed a clear oxidation peak showing typical p-type characteristics. The lowest unoccupied molecular orbital (LUMO) level was calculated from the HOMO level and optical band gap ($E_{LUMO} = E_{HOMO} + E_g$). No measurable reduction peaks were observed up to –2.0 V vs. Ag/Ag^+ in acetonitrile, suggesting strong p-type characters of the polymers. The HOMO and LUMO levels of the polymers were determined to be –5.3 ~ –5.0 eV and –3.4 ~ –3.1 eV, respectively. These values clearly show the p-type nature of the polymers due to the highly e-rich thienothiophene and weakly e-poor benzotriazole moieties. The fluorination on the BTz unit stabilized both HOMO and LUMO levels (by ca. 0.05–0.14 eV), which is consistent with the previous report [22]. The alkoxy units on the BTz unit increased both HOMO and LUMO levels (by ca. 0.16–0.26 eV) with compared to those of unsubstituted **PTTBTz**, because of electron-releasing effect of the alkoxy groups.

Thin film structure and morphology

The θ-2θ mode XRD measurement was employed to investigate molecular ordering in thin film. Polymer thin films were prepared on top of the ODTS treated SiO_2/Si substrate using chloroform or chlorobenzene solution to mimic the device fabrication process. Diffraction patterns of the polymer films are displayed in Fig. 2 as a function of annealing temperature. **PTTBTz** did not show any observable diffraction peaks in both out-of- and in-plane directions in pristine- and annealing films. In contrast, **PTTBTz-F** showed a drastic difference on molecular packing. In the pristine **PTTBTz-F** film, a pronounced diffraction pattern [showing (100) ~ (500) scattering peaks] was measured with inter-lamellar d-spacing of 18.28 Å in the out-of-plane direction. The thermal annealing increased the diffraction peak intensity (in the z direction) with the smaller inter-lamellar spacing (17.25 Å) and a π-π stacking peak (d-spacing, 3.54 Å) in the in-plane direction, showing the preferential edge-on orientation. Interestingly, some additional peaks were also observed (upon annealing) in the z direction, indicating the polycrystalline nature. The well-ordered edge-on molecular structure facilitates effective charge transport through the lateral direction along polymer stacks in the OFET device architecture. **PTTBTz-OR** also showed the edge-on orientation with well resolved out-of-plane diffraction peaks (inter-lamellar spacing, 19.19 Å) and a π-π stacking peak (d-spacing, 4.09 Å) along the in-plane direction. Introduction of fluorine or alkoxy substituents on the BTz moiety significantly impacted the intermolecular ordering through the favorable non-covalent coulombic interactions.

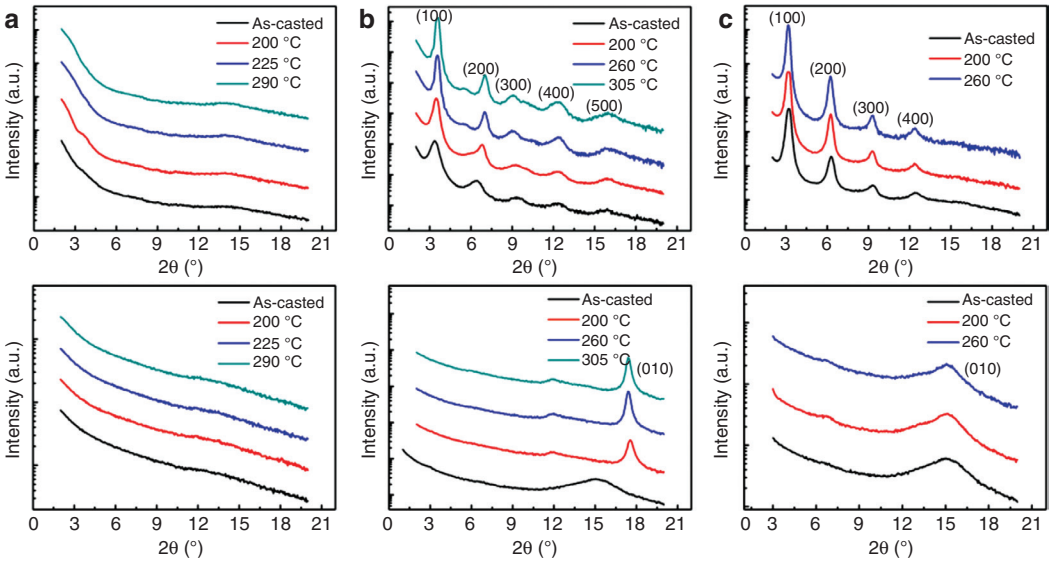

Fig. 2 Out-of -plane (top) and in-plane (bottom) X-ray diffraction of (a) **PTTBTz**, (b) **PTTBTz-F** and (c) **PTTBTz-OR** with changing the annealing temperature.

OFET properties

OFET devices were fabricated in order to characterize the charge transport properties of the BTz-based π-conjugated polymers. The extracted OFET parameters are summarized in Table 2. As shown in Fig. 3, the devices showed the typical p-channel transfer characteristics and the annealing treatments improved substantially the carrier mobility for all BTz-based copolymers.

The field-effect mobility of the as-casted **PTTBTz** film was measured to be 3.38×10^{-5} cm^2 V^{-1} s^{-1}. The fluorine substituted **PTTBTz-F** showed the hole mobility of 1.84×10^{-3} cm^2 V^{-1} s^{-1}, which is 2 orders of magnitude higher than that of **PTTBT**z. Alkoxy unit introduction also enhanced the carrier mobility by 1 order of magnitude (**PTTBTz-OR**, 5.81×10^{-4} cm^2 V^{-1} s^{-1}). The XRD data are consistent with the OFET device properties where the chemical modulation upon the BTz moiety clearly influences the intermolecular ordering and charge

Table 2 OFET characteristics of BTz-based copolymers.

Polymer	T_{ann} (°C)[a]	μ_h (cm^2 V^{-1} s^{-1})	I_{on}/I_{off}	V_{th} (V)
PTTBTz	As-cast	3.38 x 10^{-5}	4.68 x 10^2	−3.01
	130	6.37 x 10^{-5}	4.07 x 10^3	−2.12
	150	6.33 x 10^{-5}	3.93 x 10^3	−10.6
	170	2.66 x 10^{-5}	4.24 x 10^3	−14.7
PTTBTz-F	As-cast	1.84 x 10^{-3}	1.17 x 10^6	−9.21
	200	2.42 x 10^{-2}	1.23 x 10^7	−13.4
	260	3.71 x 10^{-2}	1.11 x 10^6	−18.0
	305	4.49 x 10^{-2}	1.13 x 10^7	−12.3
	320	2.97 x 10^{-2}	2.36 x 10^5	−25.9
PTTBTz-OR	As-cast	5.81 x 10^{-4}	1.19 x 10^3	13.2
	130	3.74 x 10^{-3}	5.65 x 10^3	10.2
	170	6.74 x 10^{-3}	5.60 x 10^6	9.04
	200	8.21 x 10^{-3}	3.55 x 10^4	1.64 x 10^{-3}
	260	8.39 x 10^{-3}	2.98 x 10^4	−3.07
	290	8.04 x 10^{-4}	3.14 x 10^2	−23.1

[a]T_{ann}, annealing temperature.

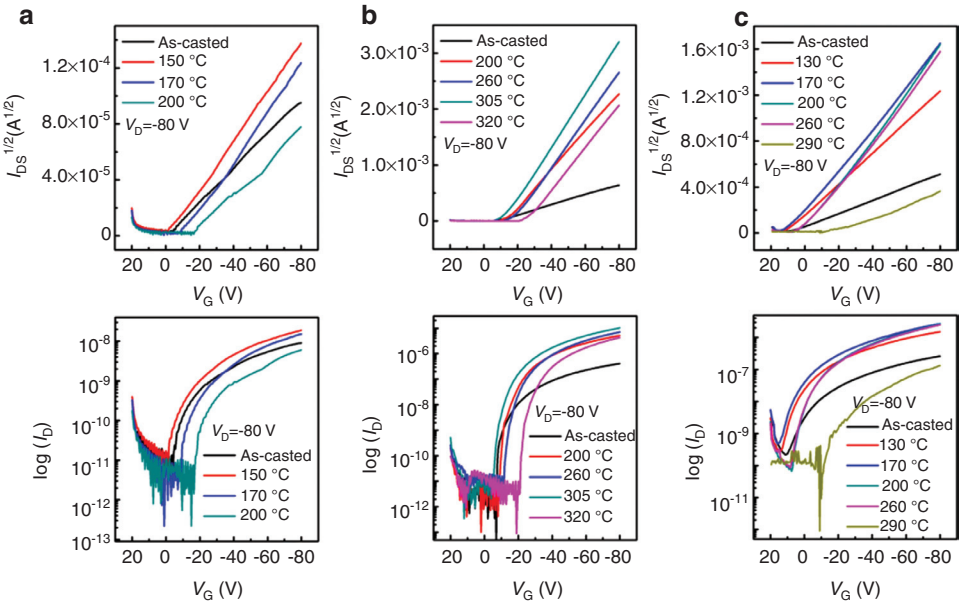

Fig. 3 Transfer characteristic of (a) **PTTBTz**, (b) **PTTBTz-F** and (c) **PTTBTz-OR**.

carrier transport characteristics. Upon thermal annealing treatments, the field-effect mobility was enhanced by approximately 2, 24, 14 times for **PTTBTz**, **PTTBTz-F** and **PTTBTz-OR**, respectively. The trend in carrier mobility is well matched with the XRD and UV-vis absorption data with changing the annealing temperature. The order of carrier mobility is as follows: **PTTBTz-F** > **PTTBTz-OR** > **PTTBTz**. The π-π stacking distance was reported to be ~3.8 Å for regio-regular P3HT [23] and the tighter π-π stacking (d = ~3.5 Å) for **PTTBTz-F** must be related to the molecular structure with intra- and interchain C-F···H, F···S and C-F···π_F non-covalent attractive interactions. These intra- and interchain hydrogen bonds and dipole-dipole coulomb interactions may significantly contribute to the well-ordered film morphology (with the shorter π-π stacking distance), resulting high interchain charge transport. Introduction of fluorine or alkoxy substituents on the BTz moiety enhanced intermolecular interaction and crystalline ordering, which was further improved by annealing processes, yielding the higher field-effect mobility with compared to the unsubstituted one. The higher degree of polymer organization was obtained with preferential edge-on orientation for **PTTBTz-F** and **PTTBTz-OR**. Finally **PTTBTz-F** (4.49×10^{-2} cm^2 V^{-1} s^{-1}) and **PTTBTz-OR** (8.39×10^{-3} cm^2 V^{-1} s^{-1}) films showed the 2~3 orders higher hole mobility than that of **PTTBTz** (6.37×10^{-5} cm^2 V^{-1} s^{-1}) after thermal annealing treatments.

The tapping mode atomic force microscopy (AFM) analyses on polymer thin films were carried out to investigate morphology of polymer films. Figure 4 displays the surface topography images with root-mean-square (rms) roughness values of the films. **PTTBTz** showed a featureless and smooth morphology with or without the annealing process. **PTTBTz-F** showed a high rms roughness value of 4.07 nm with many protrusions (probably

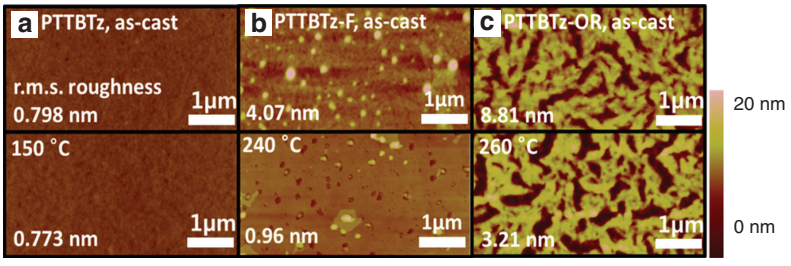

Fig. 4 AFM topography images of pristine and annealed (a) **PTTBTz**, (b) **PTTBTz-F** and (c) **PTTBTz-OR** films.

due to aggregated polymers). Upon annealing, the surface morphology became much smoother with the rms value of 0.96 nm, suggesting reorientation of polymer chains. **PTTBTz-OR** showed a very rough surface morphology for both pristine and annealed films with the high rms values (8.81 nm, 3.21 nm).

The chain linearity and planar conformation of the polymers may increase the inter-chain crystalline ordering for efficient OFET device but also lead to the chain rigidity with high degree of polymer aggregation. The homogeneous and smooth surface morphology could not be developed during film deposition for **PTTBTz-F** and **PTTBTz-OR**, because of the chain rigidity and poor solubility of the BTz-based polymers. The rough film morphology with aggregated domains disturbs the efficient charge transport along polymer crystallites [24–26]. Limited solubility of the polymers often leads to the small molecular weight of polymers, which may impede effective charge transport because of poor inter-chain connectivity. Introduction of more extended and branched side chains or siloxane-containing alkyl chains will be the solution to resolve the solubility issue and to optimize the molecular weight and film morphology for further enhancing the field-effect mobility [9].

Conclusion

Three different thienothiophene and benzotrizole-based semi-crystalline conjugated polymers were synthesized and their intermolecular ordering and field effect transistor characteristics were studied. To enhance the inter-chain ordering, the molecular structure was carefully designed by considering the backbone linearity, planarity and intra-/inter-chain non-covalent attractive interactions. Fluorine and alkoxy group substitution improved crystalline ordering which was confirmed by UV-vis absorption and X-ray diffraction measurements. The fluorine and alkoxy substituted **PTTBTz-F** and **PTTBTz-OR** showed the pronounced inter-chain packing with edge-on orientation, showing inter-lamellar spacing of 17~18 Å in the out-of-plane direction and π-π stacking (d-spacing, 3.5~4.1 Å) in the in-plane direction. The fluorine (**PTTBTz-F**: $\mu_h = 4.49 \times 10^{-2}$ cm^2 V^{-1} s^{-1}) or alkoxy (**PTTBTz-OR**: $\mu_h = 8.39 \times 10^{-3}$ cm^2 V^{-1} s^{-1}) substitution improved substantially the charge carrier mobility by 2~3 orders of magnitude, with compared to the unsubstituted **PTTBTz** ($\mu_h = 6.37 \times 10^{-5}$ cm^2 V^{-1} s^{-1}).

Acknowledgments: Yum and An contributed equally to this work. This study was supported by the National Research Foundation (NRF) Grant (2012R1A1A2005855, NRF-2009-0079630) and the Korea Foundation for the Advancement of Science & Creativity (KOFAC), and funded by the Korean Government (MOE). This work was also supported by the New & Renewable Energy Core Technology Program of the Korea Institute of Energy Technology Evaluation and Planning (KETEP), granted financial resource from the Ministry of Trade, Industry & Energy, Republic of Korea. (No. 20133030011330) and a grant (No. 2011-0031639) from the Center for Advanced Soft Electronics under the Global Frontier Research Program of the Ministry of Education, Science and Technology, Korea.

References

[1] K. J. Baeg, D. Khim, J. Kim, B. D. Yang, M. Kang, S. W. Jung, I. K. You, D. Y. Kim, Y. Y. Noh. *Adv. Funct. Mater.* **22**, 2915 (2012).
[2] A. C. Arias, S. E. Ready, R. Lujan, W. S. Wong, K. E. Paul, A. Salleo, M. L. Chabinyc, R. Apte, R. A. Street, Y. Wu, P. Liu, B. Ong. *Appl. Phys. Lett.* **85**, 3304 (2004).
[3] T. K. An, I. Kang, H.-J. Yun, H. Cha, J. Hwang, S. Park, J. Kim, Y. J. Kim, D. S. Chung, S.-K. Kwon, Y.-H. Kim, C. E. Park. *Adv. Mater.* **25**, 7003 (2013).
[4] I. Kang, H.-J. Yun, D. S. Chung, S.-K. Kwon, Y.-H. Kim. *J. Am. Chem. Soc.* **135**, 14896 (2013).
[5] T. Lei, J. H. Dou, Z. J. Ma, C. H. Yao, C. J. Liu, J. Y. Wang, J. Pei. *J. Am. Chem. Soc.* **134**, 20025 (2012).
[6] J. G. Mei, Y. Diao, A. L. Appleton, L. Fang, Z. N. Bao. *J. Am. Chem. Soc.* **135**, 6724 (2013).
[7] H. N. Tsao, D. M. Cho, I. Park, M. R. Hansen, A. Mavrinskiy, D. Y. Yoon, R. Graf, W. Pisula, H. W. Spiess, K. Mullen. *J. Am. Chem. Soc.* **133**, 2605 (2011).
[8] T. Lei, Y. Cao, X. Zhou, Y. Peng, J. Bian, J. Pei. *Chem. Mater.* **24**, 1762 (2012).

[9] J. Mei, D. H. Kim, A. L. Ayzner, M. F. Toney, Z. A. Bao. *J. Am. Chem. Soc.* **133**, 20130 (2011).
[10] H. J. Chen, Y. L. Guo, G. Yu, Y. Zhao, J. Zhang, D. Gao, H. T. Liu, Y. Q. Liu. *Adv. Mater.* **24**, 4618 (2012).
[11] I. McCulloch, M. Heeney, C. Bailey, K. Genevicius, I. Macdonald, M. Shkunov, D. Sparrowe, S. Tierney, R. Wagner, W. M. Zhang, M. L. Chabinyc, R. J. Kline, M. D. McGehee, M. F. Toney. *Nat. Mater.* **5**, 328 (2006).
[12] X. G. Guo, J. Quinn, Z. H. Chen, H. Usta, Y. Zheng, Y. Xia, J. W. Hennek, R. P. Ortiz, T. J. Marks, A. Facchetti. *J. Am. Chem. Soc.* **135**, 1986 (2013).
[13] W. Lee, H. Choi, S. Hwang, J. Y. Kim, H. Y. Woo. *Chem. Eur. J.* **18**, 2551 (2012).
[14] K. Reichenbacher, H. I. Suss, J. Hulliger. *Chem. Soc. Rev.* **34**, 22 (2005).
[15] B. Tylleman, G. Gbabode, C. Amato, C. Buess-Herman, V. Lemaur, J. Cornil, R. G. Aspe, Y. H. Geerts, S. Sergeyev. *Chem. Mater.* **21**, 2789 (2009).
[16] C. Vanpham, R. S. Macomber, H. B. Mark, H. Zimmer. *J. Org. Chem.* **49**, 5250 (1984).
[17] P. Ding, C. C. Chu, B. Liu, B. Peng, Y. P. Zou, Y. H. He, K. C. Zhou, C. S. Hsu. *Macromol. Chem. Phys.* **211**, 2555 (2010).
[18] V. N. Charushin, S. K. Kotovskaya, S. A. Romanova, O. N. Chupakhin, Y. V. Tomilov, O. M. Nefedov. *Mendeleev Commun.* **15**, 45 (2005).
[19] Z. H. Zhang, B. Peng, P. Ding, B. Liu, Y. H. He, K. C. Zhou, Y. F. Li, C. Y. Pan, Y. P. Zou. *J. Appl. Polym. Sci.* **120**, 2534 (2011).
[20] S. C. Price, A. C. Stuart, L. Q. Yang, H. X. Zhou, W. You. *J. Am. Chem. Soc* **133**, 4625 (2011).
[21] S. Yum, T. K. An, X. Wang, W. Lee, M. A. Uddin, Y. J. Kim, T. L. Nguyen, S. Xu, S. Hwang, C. E. Park, H. Y. Woo. *Chem. Mater.* **26**, 2147 (2014).
[22] H. J. Son, W. Wang, T. Xu, Y. Y. Liang, Y. E. Wu, G. Li, L. P. Yu. *J. Am. Chem. Soc.* **133**, 1885 (2011).
[23] P.-T. Wu, H. Xin, F. S. Kim, G. Ren, S. A. Jenekhe. *Macromolecules* **42**, 8817 (2009).
[24] R. J. Kline, M. D. McGehee, E. N. Kadnikova, J. S. Liu, J. M. J. Frechet, M. F. Toney. *Macromolecules* **38**, 3312 (2005).
[25] H. N. Tsao, K. Mullen. *Chem. Soc. Rev.* **39**, 2372 (2010).
[26] T. Hallam, M. Lee, N. Zhao, I. Nandhakumar, M. Kemerink, M. Heeney, I. McCulloch, H. Sirringhaus. *Phys. Rev. Lett.* **103**, 256803 (2009).